Estimating Patient Spontaneous Breathing Effort in Mechanical Ventilation Using A B-splines Function Approach

Qianhui Sun[*,], J. Geoffrey Chase[**], Cong Zhou*[*], Merryn H. Tawhai[***], Jennifer L. Knopp*[*], Knut Möller[****], Geoffrey M. Shaw[*****], Thomas Desaive[*]**

[*] *GIGA-In Silico Medicine, University of Liège, Liège, Belgium (e-mail: qianhui.sun@uliege.be; tdesaive@uliege.be)*

[**] *Department of Mechanical Engineering; Dept of Mechanical Eng, Centre for Bio-Engineering, University of Canterbury, Christchurch, New Zealand (e-mail: geoff.chase@canterbury.ac.nz; cong.zhou@canterbury.ac.nz; jennifer.knopp@canterbury.ac.nz)*

[***] *Auckland Bioengineering Institute, The University of Auckland, Auckland, New Zealand (e-mail: m.tawhai@auckland.ac.nz)*

[****] *Institute for Technical Medicine, Furtwangen University, Villingen-Schwenningen, Germany (e-mail: Knut.Moeller@hs-furtwangen.de)*

[*****] *Department of Intensive Care, Christchurch Hospital, Christchurch, New Zealand (e-mail: geoff.shaw@cdhb.health.nz)*

Abstract:

Background: Patient work of breathing is a key clinical metric strongly to guide patient care and weaning from mechanical ventilation (MV). Measurement requires added equipment, well-trained clinicians, or/and extra interventions. This study combines a spontaneous breathing effort model using b-spline functions with a nonlinear, predictive MV digital-twin model to monitor patient effort in real-time.

Methods: Data from 22 patients for two assisted spontaneous breathing MV modes, NAVA (neurally adjusted ventilatory assist) and PSV (pressure support ventilation), are employed. The patient effort function estimates a pleural pressure $\hat{P}_p$ surrogate of muscular work of breathing induced pressure. To ensure identifiability $\hat{P}_p$ is identified with a negative constraint level of 75%. Estimated patient effort is compared to electrical activity of the diaphragm (EAdi) signals from the NAVA naso-gastric tude, airway pressure, and tidal volume (V_T) as well as physiological and clinical expectations.

Results: $\hat{P}_p$ generalizes well across the digital twin model and MV modes in comparison to the original single compartment lung model. Strong neuro-muscular correlations are identified with $\hat{P}_p$ compared to EAdi, V_T, and airway pressure in NAVA. They are lower in PSV, as expected, as pressure delivery is not a function of EAdi in this MV mode, while the uncontrolled variable V_T shows a stronger association with $\hat{P}_p$ than EAdi.

Conclusion: The digital twin model relates patient-specific induced breathing effort, modeled as $\hat{P}_p$, as well as or better than EAdi in both assisted breathing MV modes. Results differ between NAVA and PSV modes due to the poorer patient-ventilator interaction typical in PSV. The ability to estimate patient work of breathing allows non-invasive, real-time quantification of ventilator unloading, heretofore not possible without extra sensors or maneuvers, to help guide weaning or changes in MV settings for assisted spontaneous breathing (ASB) MV modes.

Keywords: Electrical Activity of the Diaphragm; Patient Spontaneous Effort; Clinical Care; Digital-twin; Mechanical Ventilation; Neurally Adjusted Ventilatory Assist; Pressure Support Ventilation.

1 Introduction

The respiratory work of mechanically ventilated (MV) patients is of significant clinical interest, and is particularly relevant when gauging patient-ventilator interaction, patient-specific level of MV support, and weaning from fully supported MV to assisted spontaneous breathing (ASB) MV modes or off MV entirely [1-7]. However, under variable clinical conditions and support settings, patient spontaneous breathing can benefit or harm outcomes depending on the quality of patient-ventilator interaction [8-11]. Thus, close monitoring of patient respiratory work is needed to unveil and assess patient-ventilator synchrony to titrate ventilator support and optimize care.

Direct monitoring of respiratory electrical activity of the diaphragm muscle (EAdi), is one method to monitor and study respiratory action via multiple electrodes on the endo-tracheal tube (ETT) [12, 13]. While effective, proper positioning and regular adjustment are necessary [14, 15], requiring more clinician-involved work and training, and leading to greater variability in care and (thus) outcomes. Other clinically adopted methods, such as esophageal pressure (P_{es}) [16-18], have similar technical, and both patient and clinical burden concerns [13, 16, 19, 20]. Finally, most current methods to assess breathing effort, independent of ventilator inputs and work, still require intubation or/and additional devices, and are thus less convenient for clinical use, as well as incurring added cost and invasiveness.

WOB (work of breathing) and PTP (pressure-time product) are two popular noninvasive, mathematical signal analysis approaches. They assess respiratory effort by estimating the product of pressure-volume curves and pressure-time curves, respectively [15, 16]. Other non-invasive, derived breath effort indices can potentially offer better or equally effective respiratory muscle activities monitoring and quantification [17, 19, 21-23]. However, most of them, including WOB and PTP, recommend using P_{es} or P_{di}

(transdiaphragmatic pressure) instead of more readily available ventilator airway pressure data [16, 20], and thus still requires invasive maneuvers and/or measurements, adding cost, complexity, and risk. In particular, without these specific pressures, they cannot separate patient work of breathing and effort from the work done by the ventilator.

Clear gaps thus exist in the ability to detect and monitor patient-specific and breath-specific patient spontaneous breathing effort in an efficient, robust, and low-cost way without added invasive sensors and/or maneuvers interrupting care. While most methods require additional devices or procedures [23-27], or the required parameters are difficult to measure [22], recently proposed model-based methods offer more promise [28-31]. These studies observed correlations between ventilator support and patient work, enhancing the confidence in non-invasive, model-based procedures for estimating inspiratory work.

This study combines one of these proposed model-based estimations for patient-specific respiratory driving pressure/effort using b-spline functions [28] with a clinically proven, accurate predicting digital-twin lung mechanics model for fully supported, not spontaneously breathing, MV patients [32, 33]. The work in [28, 31] used the well-known single compartment model [34], but required specific modeling adaptations, and it cannot be easily used to understand recruitment elastance, recruited volume, distension, or asynchrony, like the digital twin model [32, 33, 35].The overall goal is to estimate patient-specific inspiratory spontaneous breathing work within the context of a proven digital twin MV patient lung mechanics model in two assisted spontaneous breathing MV modes. Successful model validation would create a framework for guiding and optimizing MV patient-ventilator interaction and care across all common forms of fully supported MV and ASB MV modes used in ICU care.

2 Methods

2.1 Patient Effort Estimation Function

This patient effort estimation model was originally developed based on the well-validated single-compartment model [36]. It adds an additional, typically negative, pressure term, $\hat{P}_p$, for pleural driving pressure due to muscular effort to estimate patient spontaneous breathing effort [28, 31]:

$$P(t) = EV(t) + RQ(t) + PEEP + \hat{P}_p \tag{1}$$

where *P(t)*, *V(t)*, and *Q(t)* are time-varying airway pressure (cmH_2O), tidal volume (L), and airway flow (L/s), respectively, which are functions of time *t* in seconds. *PEEP* is positive end expiratory pressure (cmH_2O). *E* and *R* are identified lung elastance (cmH_2O/L) and resistance ($cmH_2O/L*s^{-1}$), respectively.

The $\hat{P}_p$ term is modelled using 2nd order ($d = 2$) b-spline functions with a knot width (k_w) of 0.05 seconds to define the unknown, patient-specific $\hat{P}_p$ [28, 31]:

$$\hat{P}_p = \sum_{i=1}^{M} -P_{s,i}\Phi_{i,2}(t) \tag{2}$$

where $P_{s,i}$ are constant coefficients identified from measured data. $M = \frac{T_{insp}}{k_w} + d$ by b-spline functions setting. T_{insp} is the inspiration duration for each breath in seconds. The term $\Phi_{i,2}(t)$ using a 2nd order definition is calculated:

$$\Phi_{i,d}(t) = \frac{t - T_i}{T_{i+d} - T_i}\Phi_{i,d-1}(t) + \frac{T_{i+d+1} - t}{T_{i+d+1} - T_{i+1}}\Phi_{i+1,d-1}(t), \quad d \geq 1 \tag{3}$$

$$\Phi_{i,0}(t) = \begin{cases} 1, & T_i < t < T_i + 1 \\ 0, & otherwise \end{cases}$$

Where T_i are equally spaced division points in time calculated by $\frac{T_{insp}}{k_w}$.

Finally, Equation (1) can be written in [28]:

$$P(t) = PEEP + EV(t) + RQ(t) - \sum_{i=1}^{M} P_{s,i}\Phi_{i,2}(t) \tag{4}$$

2.2 MV Patient Digital Twin Model

To explore the efficacy and generality of this patient effort function, $\hat{P}_p$, the single-compartment model is replaced with a more complex, higher nonlinear, predictive, and clinically validated digital-twin lung mechanics model [32, 33], yielding a new model:

$$f_V(t) = P - PEEP = m\ddot{V} + R\dot{V} + K_eV + K_{h1}V_{h1} + K_{h2}V_{h2} + \sum_{i=1}^{M} -P_{s,i}\Phi_{i,2}(t) \tag{5}$$

where $f_V(t)$ is the steady-state input force, which denotes the driving pressure during breathing (*P-PEEP*). *m* represents the mass of lungs and is defined as 1 to simplify the model. *V* is the volume of air delivered to the lungs, V_{h1} and V_{h2} are hysteretic volume response during inspiration and expiration, respectively. K_e represents the alveolar recruitment elastance and *R* is the airway resistance. Specially, two nonlinear

hysteretic springs for alveolar hysteresis elastance during inspiration and expiration are defined as K_{h1} and K_{h2}, respectively. Following the settings from the prior study [28, 37], the elastances are treated to be constant across all 20 breaths for each patient and identified with R and $\hat{P}_p$ simultaneously using linear least squares regression. The digital twin model is developed from the Bouc-Wen model, and thus theoretically different from Equation (1). The detailed model development progress is available online [32, 33]. It is important to note this digital twin MV model is well-validated and can more accurately predict the outcome of changes in MV care compared to the single compartment model [32, 33, 38, 39], as well as offering better insight into patient-ventilator interaction [35, 40].

Finally, with real clinical breath data from the ventilator (*P(t), V(t), Q(t),* and *PEEP*), patient-specific, lung mechanics variables, E, R, and $\hat{P}_p$ (by identifying the $P_{s,i}$ terms) can be identified simultaneously by linear least squares regression, while constraining elements of $P_{s,i} > 0$ ($\hat{P}_p$ negative) to ensure identifiability [36, 41, 42]. An example plot for b-splines functions yielding $\hat{P}_p$ during inspiration is presented in Figure 1 with a negative constraint for $-P_{s,i}$ of 70%.

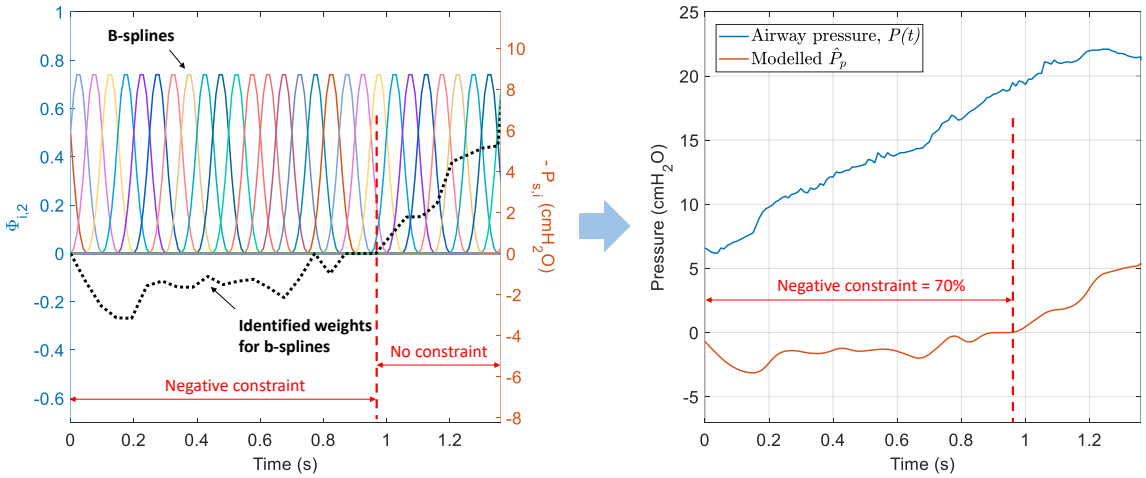

Figure 1: Examples for modelled b-splines ($\Phi_{i,2}$), identified weights for b-splines ($-P_{s,i}$), yielded $\hat{P}_p$ with associated measured airway pressure, $P(t)$, during inspiration phase. Negative constraint is 70% for $-P_{s,i}$ (and thus $\hat{P}_p$), requiring the first 70% of $P_{s,i}$ values in inspiration to be negative to ensure identifiability.

2.3 Clinical Data: NAVA and PSV

Clinical data from 22 ASB MV patients are studied. The standard patient's standard naso-gastric tube was replaced by the modified NAVA tube positioned based on the manufacturer recommendations. Airway suctioning was performed before the beginning of the protocol. The data are part of a trial on patient-ventilator synchrony at the University Hospital of Geneva (Switzerland) and Cliniques Universitaires St-Luc (Brussels, Belgium) [43].

The clinical trial included two phases, where patient data was recorded for 20 minutes (300-500 breaths) under PSV with clinician determined ventilator settings. The patient was then switched to NAVA with the NAVA level set so the peak inspiratory pressure (PIP) was similar to the level under PSV based on ventilator waveform visualization, and another 20 minutes of data was recorded. All other ventilator settings for PSV and NAVA were kept constant. During both periods, pressure, flow, and EAdi were acquired from the Servo-I ventilator through a RS232 interface and sampled at 100Hz using Servo-tracker V4.0 (Maquet Critical Care, Solna, Sweden).

2.4 Analysis and Validation

Data from the same (first) 20 breaths per patient under NAVA ventilation used in [28] are analyzed to enable model comparison between the enhanced digital twin model used here and the single compartment model used in [28]. Analyzing PSV data was not explored in [28], but provides a comparison between NAVA and the very commonly used PSV mode, and a similar first 20 breaths of data are used for consistency. This latter analysis is also the first time either lung mechanics model or a digital-twin modelling approach has been applied to PSV to the best of the authors' knowledge.

Clinical EAdi signals for both NAVA and PSV provide a reference for muscle action creating inspiratory effort. Importantly, it should be noted the EAdi signal is the input to an electro-chemical muscular reaction, which, in turn, creates diaphragm action and patient initiated inspiratory airflow. Thus, while EAdi is correlated to patient effort and resulting peak pressures and tidal volume, this correlation will only be strong if pressure is delivered based on EAdi, as in NAVA. Otherwise, the ventilator may provide greater work but at the cost of greater patient-ventilator dis-synchrony [43, 44].

2.4.1 $\hat{P}_p$ analysis

This analysis focuses on patient spontaneous breathing work estimation during inspiration. To ensure identifiability, constraints for $-P_{s,i}$ are added. In [28] the first 75% of identified $P_{s,i}$ parameters were arbitrarily constrained positive ($\hat{P}_p$ negative) and the remaining 25% was unconstrained. This negative constraint captures negative patient spontaneous breathing effort, while allowing any end-inspiratory patient resistance to ventilator action. In this study, the constraint level remains the same for consistency, but is combined with a validated predictive digital-twin model and tested with NAVA and PSV data.

2.4.2 Validation Comparisons

First, identified model fit quality is compared for NAVA with prior study using the single compartment model [28]. For both NAVA and PSV, correlations between EAdi, $\hat{P}_p$, tidal volume (V_T), and airway pressure, P_{insp}, during inspiration are considered to assess how well the non-invasively estimated $\hat{P}_p$ gauges outcome patient response to input ventilator delivery. As noted, NAVA delivers pressure based on the EAdi signal so better correlations are expected for this mode compared to PSV, which delivers a fixed pressure support regardless of patient-specific demand and has greater dis-synchrony.

3 Results

3.1 $\hat{P}_p$ Identification and Correlation

$\hat{P}_p$ identification examples using both single-compartment and digital-twin models (3 consecutive breaths from Patient 1 data under NAVA and PSV) are presented in Figure 2 with constraint levels of 75%, as in [28]. The differences are minor in terms of the shape of $\hat{P}_p$ across models, and there is no loss of fitting quality for the digital twin of Equation (5) versus the single compartment model of Equation (4) and [28]. While a larger negative area of $\hat{P}_p$ is observed in PSV compared with the NAVA, it can be observed the airway pressure and EAdi are not strongly associated in PSV.

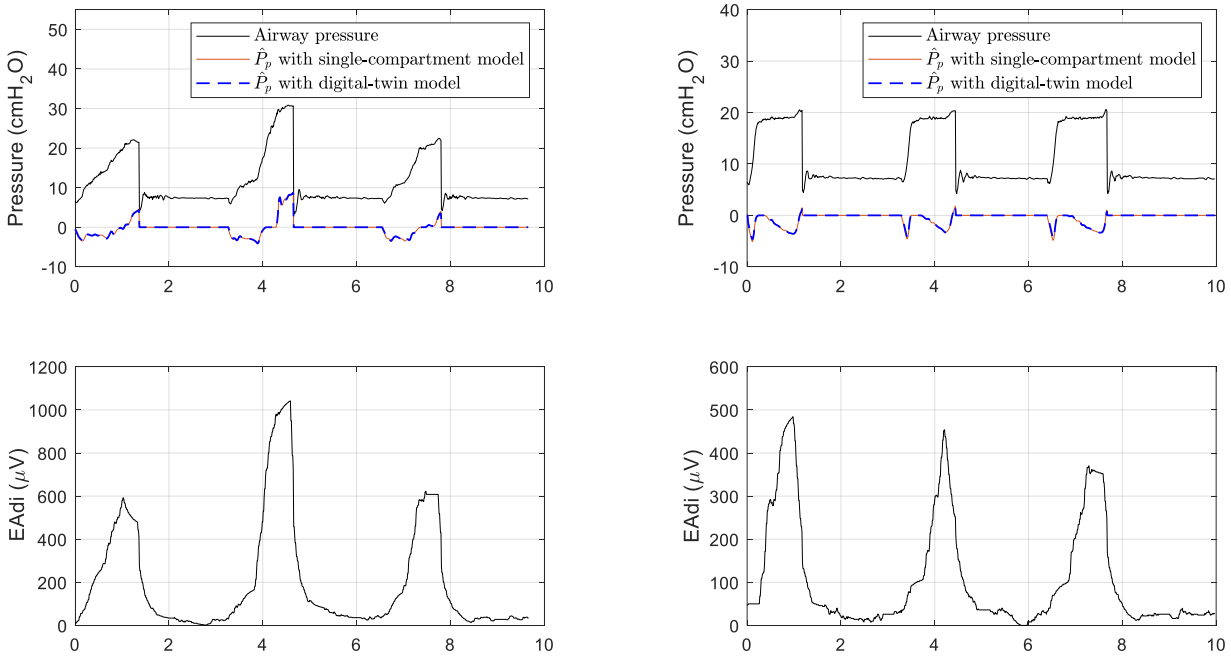

(a) NAVA (b) PSV

Figure 2: Examples for $\hat{P}_p$ identification with 3 consecutive breaths (Patient 1) for (a) NAVA and (b) PSV with negative constraint levels = 75%. Black lines for airway pressure and corresponding EAdi data. Red solid lines for identified $\hat{P}_p$ with single-compartment model, while blue dashed lines are with digital-twin model.

Correlation of the identified pleural pressure ($\hat{P}_p$) with EAdi signals, reflecting achieved negative inspiratory effort from a neural input signal yields the same median R^2 value of 0.55 (range: 0.25 and 0.86) [28], while minor difference can be observed for each patient as shown in Figure 3. Again, this result shows no loss for $\hat{P}_p$ identification quality across the two underlying lung mechanics models.

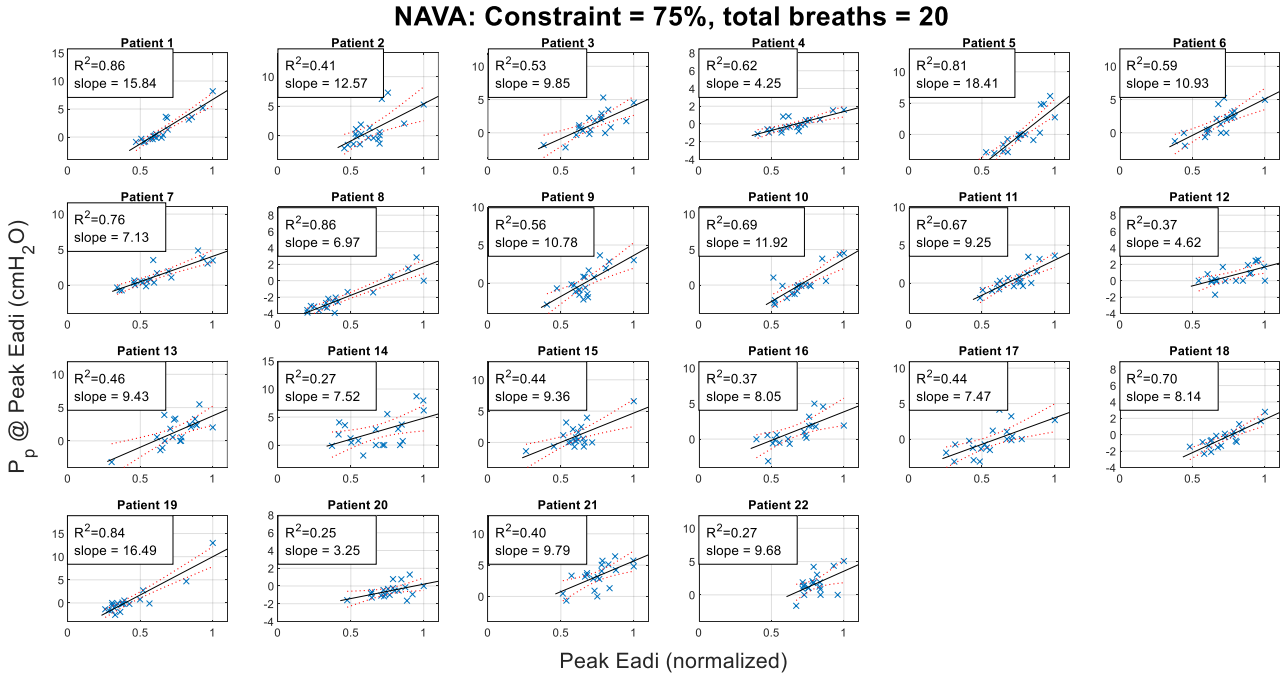

Figure 3: **NAVA, digital-twin model**: $\hat{P}_p$ values at where EAdi reaches its maximum ($\hat{P}_p|_{\text{peak EAdi}}$) versus normalized maximum EAdi values (peak EAdi) for 20 consecutive breaths for each patient at constraint level = 75%. The solid black line is the identified slope for the linear fitting. The dash red lines show the ±95% confidence level.

Table 1 shows the $\hat{P}_p$ identification outcome in NAVA. The fitting median root mean square (RMS) error is slightly lower compared to the prior study [28] with a maximum median error of 1.0 cmH_2O (was 2.3 cmH_2O). The high correlation (R^2) between PIP, peak airway pressure, and peak EAdi is expected in NAVA except for Patient 4 with $R^2 = 0.24$ (rest all ≥ 0.71). The possible reason could be misconnection with ventilator or sensor problem given the recorded airway flow has a sharp increase (near zero to the highest) within 0.04 s at the beginning of breath, available in the online Appendix.

Table 1: $\hat{P}_p$ identification outcome for **NAVA** with consecutive 20 breaths for each patient in median [IQR]. *E* and *R* are the identified elastance (cmH_2O/L) and resistance ($cmH_2O/L/s$). RMS is root mean square error (cmH_2O) for fitting. PIP is peak airway pressure. Driving pressure = PIP – PEEP. The R^2 values in the last column are the ones presented in Figure 3.

NAVA: Patient	E	R	Median RMS	Driving pressure (cmH_2O)	Peak EAdi (μV)	Peak $\hat{P}_p$ (cmH_2O)	R^2 of		
							PIP vs peak EAdi	V_T vs PIP	$\hat{P}_p$ vs peak EAdi
1	10.9	11.5	0.4	15.2 [14.3 16.8]	635 [601 716]	-3.9 [-4.1 -3.5]	0.97	0.84	0.86
2	7.2	25.5	0.2	15.8 [14.1 19.3]	417 [359 466]	-5.2 [-5.5 -4.9]	0.85	0.93	0.41
3	10.7	18.4	0.3	16.5 [14.5 18.3]	1407 [1237 1561]	-4.5 [-4.7 -4.1]	0.85	0.82	0.53
4	0.0*	2.1	0.1	2.2 [1.6 2.8]	348 [304 392]	-2.6 [-4.0 -2.4]	0.24	0.44	0.62
5	9.9	29.8	0.5	18.4 [15.4 21.7]	1947 [1617 2268]	-7.9 [-8.8 -7.3]	0.93	0.83	0.81
6	5.9	9.3	1.0	11.7 [10 12.6]	2873 [2483 3117]	-1.9 [-2.4 -1.4]	0.80	0.26	0.59
7	13.7	14.7	0.4	13.3 [10.8 16.9]	946 [780 1193]	-2.2 [-2.9 -1.9]	0.99	0.79	0.76
8	5.9	16.7	0.2	6.1 [4.1 11]	442 [324 691]	-3.8 [-4.2 -3.4]	0.99	0.96	0.86
9	19.0	25.2	0.2	24 [21 27.1]	290 [269 312]	-7.2 [-8.1 -5.9]	0.71	0.49	0.56
10	7.6	14.7	0.3	13 [11.9 14.6]	2826 [2454 3182]	-4.0 [-4.4 -3.7]	0.84	0.72	0.69
11	7.9	23.8	0.2	16.1 [13.9 19.3]	812 [675 886]	-2.7 [-3.0 -2.6]	0.92	0.87	0.67
12	14.9	17.4	0.5	13.3 [11 15.4]	1294 [1111 1559]	-2.2 [-2.9 -1.9]	0.95	0.64	0.37
13	4.8	12.6	0.8	16.6 [15.6 18]	1497 [1317 1705]	-3.4 [-4.2 -3.0]	0.87	0.44	0.46
14	8.4	14.6	0.6	16.5 [12.2 20]	985 [710 1196]	-3.8 [-4.9 -2.9]	0.87	0.72	0.27
15	17.9	16.1	0.3	22.7 [20.7 24.4]	890 [824 965]	-4.9 [-5.5 -4.5]	0.93	0.82	0.44
16	6.4	14.0	0.2	17.1 [14.4 19.7]	1513 [1184 1720]	-4.7 [-5.2 -3.8]	0.87	0.55	0.37
17	7.5	13.6	0.5	13.2 [10.8 16.3]	1395 [1129 1760]	-4.6 [-5.5 -3.2]	0.93	0.72	0.44
18	13.1	20.3	0.1	16 [13.9 17.9]	646 [570 729]	-4.1 [-4.3 -3.5]	0.92	0.53	0.70
19	17.2	21.8	0.6	16.4 [13.9 19.6]	418 [357 526]	-3.0 [-3.4 -2.7]	0.96	0.53	0.84
20	11.9	18.4	0.2	14.2 [12.6 15.6]	406 [374 449]	-2.2 [-2.5 -1.9]	0.93	0.60	0.25
21	3.9	6.0	0.5	13.2 [12 14.1]	558 [500 611]	-3.9 [-4.4 -3.4]	0.97	0.10	0.40
22	11.1	30.3	1.0	25.4 [23.4 27.5]	5240 [4809 5549]	-4.0 [-5.1 -3.7]	0.86	0.47	0.27

* The elastance identified is near zero and smaller than 0.00001, indicating irregular response to the MV modes applied, and illustrated by the irregular shape of Patient 4, which can be seen in the online Appendix. In contrast, the waveforms for Patient 5 are typical and had no such irregular values.

For PSV, the R^2 between the identified pleural pressure ($\hat{P}_p$) with EAdi signals is much lower with a median of 0.12 (range: 0.00 and 0.80) with same level of constraint, shown in Figure 4, indicating worse patient-ventilator synchronicity as observed clinically in prior studies of this cohort and others [44]. The

correlation lines are essentially around 0 slope showing no correlation due to poor patient-ventilator interaction, where the deliver fixed pressure support level overrides the patient's demand as shown in [44], and thus as expected.

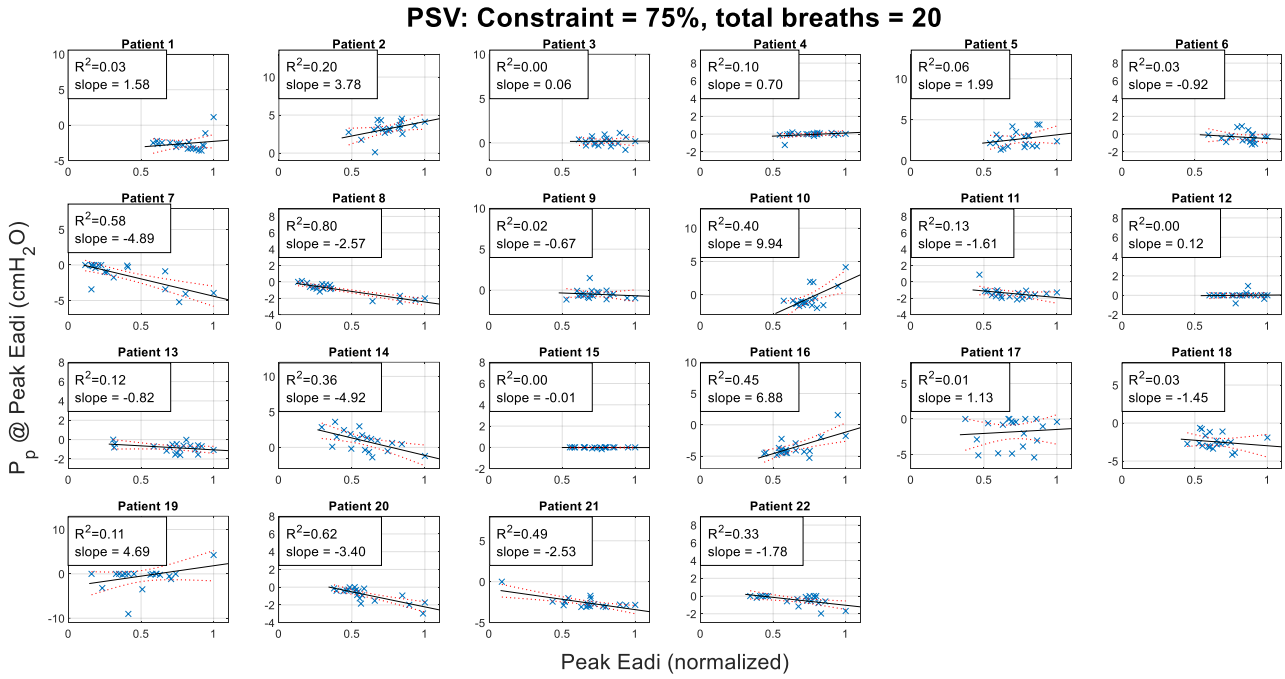

Figure 4: **PSV, digital-twin model**: $\hat{P}_p$ values at where EAdi reaches its maximum ($\hat{P}_p|_{\text{peak EAdi}}$) versus normalized maximum EAdi values (peak EAdi) for 20 consecutive breaths for each patient at constraint level = 75%. The solid black line is the identified slope for the linear fitting. The dash red lines show the ±95% confidence level.

Table 2 provides the $\hat{P}_p$ identification outcome in PSV. The low R^2 values between PIP and peak EAdi matching the clinical expectation in design for PSV (all ≤ 0.03 expect for Patient 7). The yielded $\hat{P}_p$ usually is larger than NAVA for each patient, indicating more work against ventilator by patient. Switching from NAVA to PSV, 14 patients (out of 22) experience a drop of EAdi and a more negative $\hat{P}_p$, while Patient 9 has an increase for both EAdi and $\hat{P}_p$ (less negative), matching the observed correlation in Figure 3 (positive slopes indicating smaller EAdi is associating with smaller, more negative, $\hat{P}_p$).

Note that in NAVA, the breath support from patient is proportional to EAdi signals while in PSV the support is fixed. The elastance and resistance identification outcomes for Patient 4 are different between NAVA and PSV modes, shown in Tables 1-2. It probably shows a level of worse condition for Patient 4 compared to other patients, particularly in response to MV care, as indicated by the irregular respiratory waveforms in the online Appendix.

Table 2: $\hat{P}_p$ identification outcome for **PSV** with consecutive 20 breaths for each patient in median [IQR]. *E* and *R* are the identified elastance (cmH_2O/L) and resistance ($cmH_2O/L/s$). RMS is root mean square error for fitting. PIP is peak airway pressure. Driving pressure = PIP – PEEP. The R^2 values in the last column are the ones presented in Figure 4.

PSV: Patient	E	R	Median RMS	Driving pressure (cmH_2O)	Peak EAdi (μV)	Peak $\hat{P}_p$ (cmH_2O)	R^2 of		
							PIP vs peak EAdi	Vt vs PIP	$\hat{P}_p$ vs peak EAdi
1	13.0	13.5	0.6	13.3 [13.2 13.4]	436 [381 479]	-4.3 [-4.4 -4.1]	0.08	0.05	0.03
2	7.9	19.2	1.0	14.9 [14.8 14.9]	1294 [1162 1430]	-6.2 [-6.5 -5.3]	0.25	0.50	0.20
3	11.7	18.9	0.3	14.2 [14.1 14.2]	1340 [1208 1460]	-5.6 [-5.9 -5.5]	0.07	0.07	0.00
4	5.0	6.8	0.2	5.2 [5.1 5.3]	272 [217 283]	-6.9 [-7.1 -6.6]	0.02	0.02	0.10
5	11.8	25.5	0.2	17 [16.9 17.3]	2263 [1888 2482]	-9.1 [-9.3 -8.9]	0.00	0.00	0.06
6	9.2	12.4	0.7	10.8 [10.7 10.9]	1342 [1186 1385]	-2.8 [-3.1 -2.6]	0.04	0.37	0.03
7	16.4	21.1	0.5	9.8 [9.8 10.1]	359 [247 812]	-4.2 [-4.4 -4.0]	0.79	0.50	0.58
8	5.4	14.0	0.1	8.1 [7.7 8.3]	217 [176 357]	-4.0 [-4.3 -3.9]	0.05	0.18	0.80
9	17.5	25.7	0.2	16.9 [16.9 17]	532 [493 614]	-6.4 [-6.5 -6.2]	0.03	0.31	0.02
10	9.4	16.9	0.2	13.2 [13.2 13.3]	2407 [2274 2596]	-3.6 [-3.7 -3.4]	0.01	0.01	0.40
11	12.9	23.9	0.2	17.1 [17 17.2]	816 [733 976]	-6.0 [-6.1 -5.5]	0.01	0.01	0.13
12	18.9	24.6	0.7	14.3 [14.3 14.3]	1939 [1723 2137]	-6.0 [-6.2 -5.3]	0.00	0.01	0.00
13	7.5	17.9	0.6	15.2 [15.2 15.2]	933 [848 1057]	-4.1 [-4.3 -4.0]	0.00	0.13	0.12
14	11.7	26.3	0.4	17.1 [16.8 17.3]	419 [338 475]	-6.5 [-7.0 -6.0]	0.01	0.03	0.36
15	20.1	15.5	0.5	16.1 [16.1 16.1]	640 [555 683]	-12.1 [-12.2 -11.9]	0.00	0.04	0.00
16	10.8	17.5	0.3	13.6 [13.6 13.8]	1015 [953 1265]	-4.7 [-4.9 -4.4]	0.05	0.06	0.45
17	11.2	20.7	0.9	14.6 [14.5 14.7]	687 [606 804]	-5.4 [-5.6 -5.1]	0.34	0.17	0.01
18	18.6	25.6	0.3	15.5 [15.5 15.6]	603 [552 687]	-9.2 [-9.4 -8.8]	0.30	0.22	0.03
19	17.1	21.3	1.1	16.7 [16.3 17.3]	747 [576 935]	-6.7 [-7.3 -6.3]	0.01	0.06	0.11
20	13.4	22.2	0.1	12.9 [12.9 13]	252 [224 289]	-3.6 [-3.9 -3.4]	0.04	0.16	0.62
21	6.9	9.5	0.4	9.3 [9.2 9.4]	502 [393 556]	-3.4 [-3.6 -3.1]	0.15	0.25	0.49
22	7.8	22.4	1.0	15.9 [15.9 15.9]	5047 [3156 5481]	-6.0 [-6.6 -5.7]	0.09	0.16	0.33

3.2 Pleural Pressure ($\hat{P}_p$) versus EAdi Signal with Breath Data

Figure 5 shows mean values for airway pressure during inspiration (P_{insp}) and identified pleural pressure, $\hat{P}_p$, for the same 20 breaths data analyzed in Figure 3. Figure 6 shows these values for PSV. The dashed diagonal lines are constant iso-transpulmonary pressure, iso-P_{tp} with slope = 1 [45] showing an expected consistent value during NAVA, which, again, bases pressure delivery on EAdi, where PSV in Figure 6 does not, and results in greater dys-synchrony between patient-specific demand and support. For NAVA in Figure 5 most patients close to the iso-P_{tp}, with tight 95% confidence level. Thus, these figures suggest overall breath-breath consistency in neuromuscular coupling for NAVA, but less so, as expected for PSV, where mean inspiratory pressure is largely constant as PSV provides the same pressure regardless of patient-specific EAdi-assessed demand [43, 44, 46].

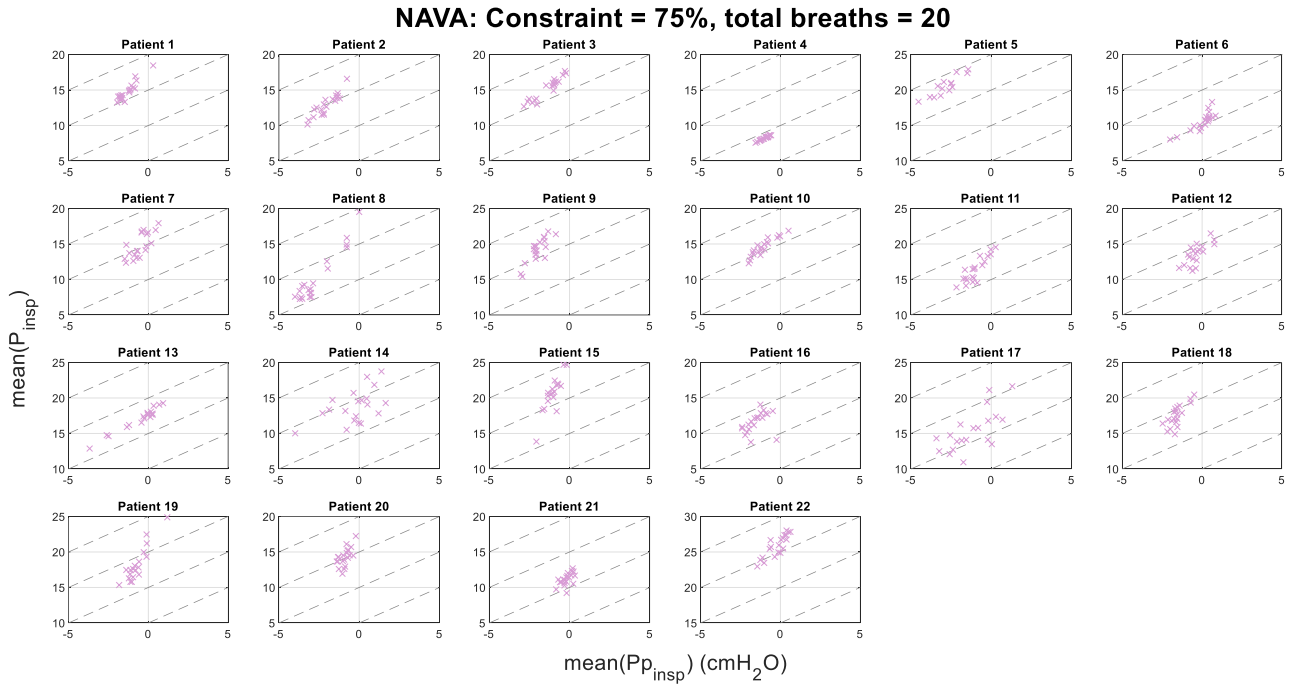

Figure 5: The mean values of airway pressure (P_{insp}) versus the mean values of the identified pleural pressure $\hat{P}_p$ during inspiration for 20 consecutive breaths for each patient at constraint level = 75% (**NAVA, digital-twin model**). Dashed diagonal lines represent the iso-transpulmonary pressure (P_{tp}) [45].

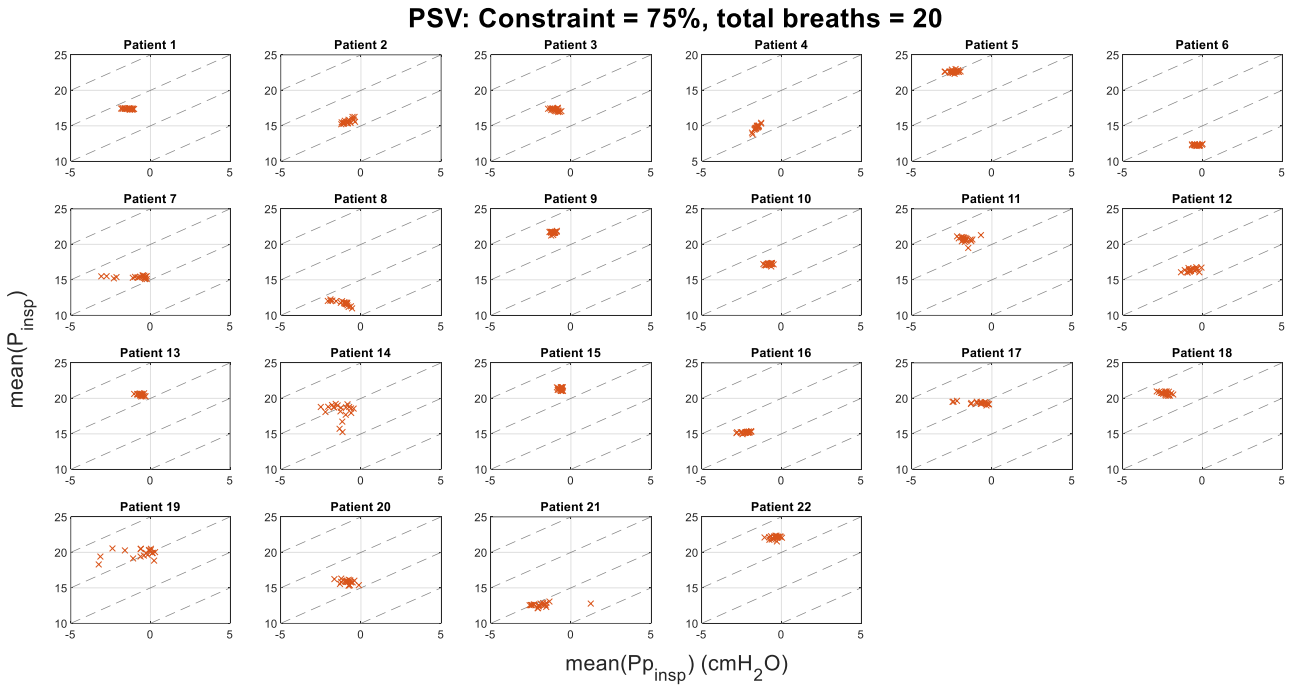

Figure 6: The mean values of airway pressure (P_{insp}) versus the mean values of the identified pleural pressure $\hat{P}_p$ during inspiration for 20 consecutive breaths for each patient at constraint level = 75% (**PSV, digital-twin model**). Dashed diagonal lines represent the iso-transpulmonary pressure (P_{tp}) [45].

Given that EAdi measures the diaphragm activity which could have minor fluctuations by time and be influenced by possible asynchrony, the mean value of it during inspiration, mean(EAdi), is considered to be more robust to present the diaphragm activity level for patients. Thus, the identified pleural pressure is also analyzed in mean values here, mean($\hat{P}_p$). Then, their correlations towards two of the most important ventilator breath variables, PIP and V_T. are studied and provided in Table 3. In NAVA, a high correlation in mean(EAdi) with PIP is observed (median [IQR]: 0.70 [0.44 0.79]) and expected since its delivered airway pressure is designed to be proportional to EAdi signals, while mean($\hat{P}_p$) also yielded a good correlation (0.51 [0.27 0.67]). Meanwhile, the uncontrolled V_T has relatively lower R^2 values with both $\hat{P}_p$ and EAdi, with a median of 0.37 and 0.43, respectively.

In poorer patient-ventilator interaction mode, PSV, the amount of delivery pressure is fixed (seen in Table

2 and Figure 2) which thus leads to the low R^2 towards PIP. As for V_T, $\hat{P}_p$ shows a great improvement to EAdi with an average increase of 0.28 for 20 patients (out of 22).

Table 3: Breath data, PIP and V_T, versus the mean of pleural pressure $\hat{P}_p$ and diaphragm muscle activity EAdi during inspiration for **NAVA** and **PSV**. R^2 values are presented per patient and in overall median and IQR.

Patient	**NAVA**				**PSV**			
	PIP vs mean($\hat{P}_p$)	V_T vs mean($\hat{P}_p$)	PIP vs mean(EAdi)	V_T vs mean(EAdi)	PIP vs mean($\hat{P}_p$)	V_T vs mean($\hat{P}_p$)	PIP vs mean(EAdi)	V_T vs mean(EAdi)
1	0.67	0.78	0.93	0.82	0.02	0.86	0.22	0.32
2	0.58	0.48	0.43	0.30	0.34	0.17	0.35	0.66
3	0.65	0.71	0.79	0.75	0.27	0.34	0.08	0.11
4	0.24	0.48	0.16	0.22	0.03	0.51	0.05	0.06
5	0.78	0.61	0.71	0.64	0.17	0.06	0.00	0.01
6	0.63	0.01	0.68	0.02	0.16	0.69	0.03	0.02
7	0.32	0.14	0.78	0.70	0.85	0.72	0.84	0.43
8	0.91	0.85	0.95	0.97	0.17	0.94	0.09	0.88
9	0.36	0.28	0.50	0.39	0.04	0.14	0.04	0.04
10	0.47	0.36	0.74	0.62	0.06	0.45	0.01	0.00
11	0.75	0.55	0.48	0.37	0.05	0.17	0.12	0.01
12	0.34	0.35	0.73	0.76	0.13	0.05	0.00	0.01
13	0.79	0.47	0.77	0.38	0.22	0.61	0.00	0.30
14	0.26	0.06	0.30	0.22	0.10	0.52	0.02	0.42
15	0.63	0.76	0.84	0.70	0.16	0.12	0.01	0.34
16	0.23	0.01	0.67	0.40	0.05	0.09	0.02	0.04
17	0.35	0.16	0.79	0.53	0.05	0.88	0.51	0.31
18	0.55	0.24	0.36	0.24	0.29	0.04	0.34	0.00
19	0.84	0.38	0.94	0.48	0.34	0.24	0.00	0.06
20	0.23	0.04	0.65	0.40	0.28	0.88	0.19	0.02
21	0.16	0.47	0.13	0.20	0.18	0.75	0.26	0.53
22	0.25	0.19	0.43	0.46	0.11	0.21	0.06	0.02
Median IQR	0.51 [0.27 0.67]	0.37 [0.17 0.54]	0.70 [0.44 0.79]	0.43 [0.32 0.68]	0.16 [0.05 0.26]	0.40 [0.14 0.71]	0.05 [0.01 0.21]	0.06 [0.02 0.34]

4 Discussion

4.1 The Outcome

In the studied clinical trial, two different ventilation modes are applied to the same 22 patients, NAVA and PSV. The differences between MV modes can be observed in Figure 2 where $\hat{P}_p$ yield larger and less regular negative area in PSV under the same constraint setting for same patient. The R^2 values studied in prior work ($\hat{P}_p$ values at where EAdi reaches its maximum versus peak EAdi) yielded a median of 0.55 and IQR = 0.38-0.70 at constraint = 75% [28]. With the digital-twin model, Equation (5), the overall $\hat{P}_p$ identification is similar and yields a median of 0.55 and IQR = 0.40-0.70 at same constraint level, shown in Figure 3, showing the great neuromuscular coupling performance observed in NAVA, which meets this clinical expectation by design. Figure 4 shows the same analysis for PSV and it yields a much lower correlation, as expected in clinical. The inconsistent slopes (positive or negative for different patients) are presenting the lack of patient specificity and meets the observations in [44, 47, 48].

In general, patient spontaneous work, estimating and representing by $\hat{P}_p$ and EAdi signals, can vary based on the patient's need and ability to breath, and is thus quite variable breath-to-breath [31, 44]. As a result, the shape and peak values of EAdi signals are different, in results and Appendix, given on the intensity of suppression of patient spontaneous effort, where NAVA is less and PSV is stronger. PSV mode delivers a step input and NAVA delivers a ramp in terms of total pressure support [44, 49]. It thus illustrates the lower EAdi peak values in PSV than NAVA and these differences also lead to different elastic responses [49]. As a result, the variation of $\hat{P}_p$ and EAdi signals across breaths and patients can be seen in the results and Appendix. This variability has many factors, including ventilator unloading due to excess support and intra-patient variability in demand as well as in response to the different MV modes delivery of support.

The great consistency between identified $\hat{P}_p$ and physiological response from patient (constant iso-transpulmonary pressure, iso-P_{tp} [45]) is shown in Figure 5 for NAVA. The alignment of mean(P_{insp}) and mean($\hat{P}_p$) towards the constant iso-P_{tp} [45] suggests a close interaction between $\hat{P}_p$, the neural respiratory feedback mechanisms, and the EAdi output. Figure 6 offers the same analysis for PSV. Again, low correlation is observed in PSV. It is reasonable that PSV, compared with NAVA ventilation based on measured EAdi signals for proportional patients assist, simply delivers airway flow up to a targeted driving pressure (PIP - PEEP), can be compared in Tables 1-2 and Figure 2, where the delivered pressure is strictly fixed and loses the interaction with neural respiratory feedback and EAdi.

Those low correlation values match expectations from prior studies for PSV [44, 47, 48], and as a result of observed poorer patient-ventilator interaction [43]. There is thus significant mismatch in PSV between inspiratory effort measured by EAdi and the uncontrolled variable, tidal volume, achieved amongst the 22 patients [43, 44, 47, 48]. This mismatch yields a correspondingly lower correlation, as expected and discussed, between inspiratory effort identified, or measured via EAdi, and outcome work of breathing or tidal volume. Hence, the overall comparison shows identification of patient effort for PSV would be a more challenging work in clinical.

In PSV, the more variable performance (variable patient drive) and the low consistency between patient respiratory drive, $\hat{P}_p$, and EAdi signals are observed with the low R^2 values in Figure 4 and Table 2. The yielded $\hat{P}_p$ in PSV usually is larger (more negative) than NAVA for each patient, indicating stronger resist against ventilator support. Switching from NAVA to PSV, 14 patients yielded a more negative $\hat{P}_p$ with a change (drop) range from 0.1 to 7.2 cmH_2O; 14 patients (not same group with $\hat{P}_p$ drop) are observed with

a drop in driving pressure (range: 0.4 – 9.5 cmH_2O); 16 patients have a drop in peak EAdi (range: 43 – 1531 μV). Finally, 10 out of 22 patients have a drop in all driving pressure, peak EAdi, and $\hat{P}_p$, may showing a better neuro-muscular correlation than other patients, matching the examples for good neuro-muscular correlation in Figure 3 in NAVA, where smaller the EAdi signal, more negative $\hat{P}_p$ yields. This overall performance shows the variable behavior of PSV patients.

Meanwhile, the monitored EAdi signals do not have a noticeable correlation with PIP or V_T in PSV, shown in Table 3, with median R^2 of 0.05 and 0.06, respectively. Meanwhile, a stronger correlation association is yielded with $\hat{P}_p$ and V_T. 20 patients (out of 22) are having a larger R^2 values with an average increase (ΔR^2) of 0.28, and yielded a new median R^2 value of 0.48 (IQR = 0.16 – 0.73) compared with the median of 0.05 and IQR = 0.02 - 0.32 in mean(EAdi) versus V_T. Only 2 patients have a decrease of R^2 (Patients 2 and 15). The overall increasement is invisible and stronger, showing a better association between the uncontrollable variable V_T and pleural pressure $\hat{P}_p$ than EAdi signals in PSV.

4.2 Main Contribution

To conclude, this study tested a patient effort estimation function, b-splines function $\hat{P}_p$, and combined with a validated digital-twin model with both NAVA and PSV data. Same constraint level for $\hat{P}_p$ is tested from prior study and showing no fitting loss when combined with the digital-twin model. Meanwhile, this study compared NAVA and PSV data, showing the great neuro-muscular correlation in NAVA and the more variable performance of PSV patients under similar pressure support setting. The analysis across $\hat{P}_p$, airway pressure, and iso-P_{tp} presents the great association between patient physiological response with $\hat{P}_p$ in NAVA.

This work firstly combined the b-splines function with a predictive lung mechanics model to identify pleural pressure $\hat{P}_p$, enhanced the capability and validated the generality of b-spline functions. It first time employed the b-splines function with PSV data to identify patient effort and compared with EAdi signals. Physiological correlations between $\hat{P}_p$ and respiratory system feedback are analyzed. Finally, $\hat{P}_p$ shows a great improvement in correlation towards the variable, unpredictable V_T in PSV than EAdi.

Furthermore, great generality is validated between two lung mechanics models, the single compartment model and the predictive digital twin model. While some works with single compartment model have good prediction [40], it is less accurate and less robust across patients and MV modes. Furthermore, digital twin model can add terms to account for over-distension (high lung injury risks) index [33] and identify asynchrony breaths [50] in clinical care. The single compartment model is less capable in both regards. Hence, the combination of predictive digital twin model and patient spontaneous effort estimation function $\hat{P}_p$ offers more promising use and capability in future work and clinical care.

5 Conclusion

In conclusion, the studied b-splines function model for inspiratory effort generalizes well between the two lung mechanics models considered, and its efficacy for the digital-twin model is promising for creating a more general overall model-based approach to MV monitoring and care. Thus, model generalizability is demonstrated with minimal added constraint for $\hat{P}_p$ to ensure identifiability. Further, strong neuro-muscular consistency is observed by $\hat{P}_p$ in NAVA than PSV. Stronger correlation with tidal volume in PSV (poor patient-ventilator interaction) with $\hat{P}_p$ than EAdi is observed. The b-splines function for estimating patient respiratory work is worthy to explore more and deeper for future clinical decision aid.

6 Acknowledgement

This work was supported the NZ Tertiary Education Commission (TEC) fund MedTech CoRE (Centre of Research Excellence; #3705718), the NZ National Science Challenge 7, Science for Technology and Innovation (2019-S3-CRS), and the Service Public Fédéral Stratégie et Appui (BOSA) – DIGITWIN4PH.

REFERENCES

1. Haas, C.F., Mechanical Ventilation with Lung Protective Strategies: What Works? *Critical Care Clinics* (2011). p. 469-486, http://linkinghub.elsevier.com/retrieve/pii/S0749070411000297?showall=true.
2. Patel, D.S., Rafferty, G.F., Lee, S., Hannam, S., and Greenough, A., Work of breathing during SIMV with and without pressure support. *Archives of Disease in Childhood* (2009). p. 434-436 DOI: 10.1136/adc.2008.152926.
3. Tobin, M.J., Jubran, A., and Laghi, F., Patient-Ventilator Interaction. *Am. J. Respir. Crit. Care Med.* (2001). p. 1059-1063, http://ajrccm.atsjournals.org.
4. Tobin, M.J., Physiologic basis of mechanical ventilation. *Annals of the American Thoracic Society* (2018). p. S49-S52.
5. Navalesi, P., Bruni, A., Garofalo, E., Biamonte, E., Longhini, F., and Frigerio, P., Weaning off mechanical ventilation: much less an art, but not yet a science. *Annals of translational medicine* (2019).
6. van Dijk, J., Koopman, A.A., de Langen, L.B., Dijkstra, S., Burgerhof, J.G., Blokpoel, R.G., and Kneyber, M.C., Effect of pediatric ventilation weaning technique on work of breathing. (2022).
7. Zein, H., Baratloo, A., Negida, A., and Safari, S., Ventilator weaning and spontaneous breathing trials; an educational review. *Emergency* (2016). p. 65.
8. Mauri, T., Cambiaghi, B., Spinelli, E., Langer, T., and Grasselli, G., Spontaneous breathing: a double-edged sword to handle with care. *Ann Transl Med* (2017). p. 292 DOI: 10.21037/atm.2017.06.55.
9. Yoshida, T., Grieco, D.L., Brochard, L., and Fujino, Y., Patient self-inflicted lung injury and positive end-expiratory pressure for safe spontaneous breathing. *Curr Opin Crit Care* (2020). p. 59-65 DOI: 10.1097/mcc.0000000000000691.
10. Yoshida, T., Fujino, Y., Amato, M.B.P., and Kavanagh, B.P., Fifty Years of Research in ARDS. Spontaneous Breathing during Mechanical Ventilation. Risks, Mechanisms, and Management. *American Journal of Respiratory and Critical Care Medicine* (2017). p. 985-992 DOI: 10.1164/rccm.201604-0748CP.
11. de Vries, H., Jonkman, A., Shi, Z.H., Spoelstra-de Man, A., and Heunks, L., Assessing breathing effort in mechanical ventilation: physiology and clinical implications. *Ann Transl Med* (2018). p. 387 DOI: 10.21037/atm.2018.05.53.
12. Fan, E., Villar, J., and Slutsky, A.S., Novel approaches to minimize ventilator-induced lung injury. *BMC medicine* (2013). p. 1-9.
13. Jonkman, A.H., de Vries, H.J., and Heunks, L.M.A., Physiology of the Respiratory Drive in ICU Patients: Implications for Diagnosis and Treatment. *Critical Care* (2020). p. 104 DOI: 10.1186/s13054-020-2776-z.
14. Vargas, M., Buonanno, P., Sica, A., Ball, L., Iacovazzo, C., Marra, A., Pelosi, P., and Servillo, G., Patient-Ventilator Synchrony in Neurally-Adjusted Ventilatory Assist and Variable Pressure Support Ventilation. *Respir Care* (2022). p. 503-509 DOI: 10.4187/respcare.08921.
15. Cross, T.J., Isautier, J.M.J., Kelley, E.F., Hubbard, C.D., Morris, S.J., Smith, J.R., and Duke, J.W., A Systematic Review of Methods Used to Determine the Work of Breathing during Exercise. *Med Sci Sports Exerc* (2023). p. 1672-1682 DOI: 10.1249/mss.0000000000003187.
16. Akoumianaki, E., Maggiore, S.M., Valenza, F., Bellani, G., Jubran, A., Loring, S.H., Pelosi, P., Talmor, D., Grasso, S., Chiumello, D., Guérin, C., Patroniti, N., Ranieri, V.M., Gattinoni, L., Nava, S., Terragni, P.-P., Pesenti, A., Tobin, M., Mancebo, J., and Brochard, L., The Application of

Esophageal Pressure Measurement in Patients with Respiratory Failure. *American Journal of Respiratory and Critical Care Medicine* (2014). p. 520-531 DOI: 10.1164/rccm.201312-2193CI.

17. Telias, I. and Savino, S., Techniques to monitor respiratory drive and inspiratory effort. *Current Opinion in Critical Care* (2019). p. 1 DOI: 10.1097/MCC.0000000000000680.
18. Mauri, T., Yoshida, T., Bellani, G., Goligher, E.C., Carteaux, G., Rittayamai, N., Mojoli, F., Chiumello, D., Piquilloud, L., Grasso, S., Jubran, A., Laghi, F., Magder, S., Pesenti, A., Loring, S., Gattinoni, L., Talmor, D., Blanch, L., Amato, M., Chen, L., Brochard, L., Mancebo, J., and the, P.p.w.G., Esophageal and transpulmonary pressure in the clinical setting: meaning, usefulness and perspectives. *Intensive Care Medicine* (2016). p. 1360-1373 DOI: 10.1007/s00134-016-4400-x.
19. Jansen, D., Jonkman, A.H., Roesthuis, L., Gadgil, S., van der Hoeven, J.G., Scheffer, G.-J.J., Girbes, A., Doorduin, J., Sinderby, C.S., and Heunks, L.M.A., Estimation of the diaphragm neuromuscular efficiency index in mechanically ventilated critically ill patients. *Critical Care* (2018). p. 238 DOI: 10.1186/s13054-018-2172-0.
20. Pierantonio, L., Andre, A., Andrea, A., Tony, B., Esther, B., Martin, D., Bruno-Pierre, D., Brigitte, F., Joaquim, G., Jordan, A.G., Anna, L.H., Hans-Joachim, K., Franco, L., Daniel, L., Yuan-Ming, L., Neder, J.A., Denis, O., Donnell, Michael, I.P., Roberto , A.R., Andrea, R., Frédéric, S., Thomas, S., Christina, M.S., Ioannis, V., and Samuel, V., ERS statement on respiratory muscle testing at rest and during exercise. *European Respiratory Journal* (2019). p. 1801214 DOI: 10.1183/13993003.01214-2018.
21. Jonkman, A.H., Jansen, D., Gadgil, S., Keijzer, C., Girbes, A.R.J., Scheffer, G.-J., Hoeven, J.G.v.d., Tuinman, P.R., Man, A.M.E.S.-d., Sinderby, C.S., and Heunks, L.M.A., Monitoring patient-ventilator breath contribution in the critically ill during neurally adjusted ventilatory assist: reliability and improved algorithms for bedside use. *Journal of Applied Physiology* (2019). p. 264-271 DOI: 10.1152/japplphysiol.00071.2019.
22. Telias, I., Junhasavasdikul, D., Rittayamai, N., Piquilloud, L., Chen, L., Ferguson, N.D., Goligher, E.C., and Brochard, L., Airway Occlusion Pressure As an Estimate of Respiratory Drive and Inspiratory Effort during Assisted Ventilation. *American Journal of Respiratory and Critical Care Medicine* (2020). p. 1086-1098 DOI: 10.1164/rccm.201907-1425OC.
23. Campoccia Jalde, F., Jalde, F., Wallin, M.K.E.B., Suarez-Sipmann, F., Radell, P.J., Nelson, D., Eksborg, S., and Sackey, P.V., Standardized Unloading of Respiratory Muscles during Neurally Adjusted Ventilatory Assist: A Randomized Crossover Pilot Study. *Anesthesiology* (2018). p. 769-777 DOI: 10.1097/ALN.0000000000002335.
24. Bellani, G., Mauri, T., Coppadoro, A., Grasselli, G., Patroniti, N., Spadaro, S., Sala, V., Foti, G., and Pesenti, A., Estimation of Patient's Inspiratory Effort From the Electrical Activity of the Diaphragm*. *Critical Care Medicine* (2013), https://journals.lww.com/ccmjournal/Fulltext/2013/06000/Estimation_of_Patient_s_Inspiratory_Effort_From.12.aspx.
25. van Diepen, A., Bakkes, T., De Bie, A.J.R., Turco, S., Bouwman, R.A., Woerlee, P.H., and Mischi, M., Evaluation of the accuracy of established patient inspiratory effort estimation methods during mechanical support ventilation. *Heliyon* (2023). p. e13610 DOI: 10.1016/j.heliyon.2023.e13610.
26. Graßhoff, J., Petersen, E., Walterspacher, S., and Rostalski, P., Model-Based Estimation of Inspiratory Effort Using Surface EMG. *IEEE Transactions on Biomedical Engineering* (2023). p. 247-258 DOI: 10.1109/TBME.2022.3188183.
27. Lassola, S., Miori, S., Sanna, A., Menegoni, I., De Rosa, S., Bellani, G., and Umbrello, M. *Assessment of Inspiratory Effort in Spontaneously Breathing COVID-19 ARDS Patients Undergoing Helmet CPAP: A Comparison between Esophageal, Transdiaphragmatic and Central*

Venous Pressure Swing. Diagnostics, 2023. **13**, DOI: 10.3390/diagnostics13111965.
28. Knopp, J.L., Chase, J.G., Kim, K.T., and Shaw, G.M., Model-based estimation of negative inspiratory driving pressure in patients receiving invasive NAVA mechanical ventilation. *Comput Methods Programs Biomed* (2021). p. 106300 DOI: 10.1016/j.cmpb.2021.106300.
29. Chiew, Y.S., Chase, J., Lambermont, B., Roeseler, J., Bialais, E., Sottiaux, T., and Desaive, T., Effects of Neurally Adjusted Ventilatory Assist (NAVA) levels in non-invasive ventilated patients: Titrating NAVA levels with electric diaphragmatic activity and tidal volume matching. *Biomedical engineering online* (2013). p. 61 DOI: 10.1186/1475-925X-12-61.
30. Damanhuri, N.S., Chiew, Y.S., Othman, N.A., Docherty, P.D., Pretty, C.G., Shaw, G.M., Desaive, T., and Chase, J.G., Assessing respiratory mechanics using pressure reconstruction method in mechanically ventilated spontaneous breathing patient. *Computer Methods and Programs in Biomedicine* (2016). p. 175-185 DOI: https://doi.org/10.1016/j.cmpb.2016.03.025.
31. Guy, E.F.S., Chase, J.G., Knopp, J.L., and Shaw, G.M., Quantifying ventilator unloading in CPAP ventilation. *Computers in Biology and Medicine* (2022). p. 105225 DOI: https://doi.org/10.1016/j.compbiomed.2022.105225.
32. Zhou, C., Chase, J.G., Knopp, J., Sun, Q., Tawhai, M., Möller, K., Heines, S.J., Bergmans, D.C., Shaw, G.M., and Desaive, T., Virtual patients for mechanical ventilation in the intensive care unit. *Computer Methods and Programs in Biomedicine* (2021). p. 105912 DOI: https://doi.org/10.1016/j.cmpb.2020.105912.
33. Sun, Q., Chase, J.G., Zhou, C., Tawhai, M.H., Knopp, J.L., Möller, K., and Shaw, G.M., Over-distension prediction via hysteresis loop analysis and patient-specific basis functions in a virtual patient model. *Computers in Biology and Medicine* (2021). p. 105022 DOI: https://doi.org/10.1016/j.compbiomed.2021.105022.
34. Bates, J.H. *Pulmonary mechanics: a system identification perspective*. in *2009 Annual International Conference of the IEEE Engineering in Medicine and Biology Society*. 2009. IEEE.
35. Zhou, C., Chase, J.G., Sun, Q., Knopp, J., Tawhai, M.H., Desaive, T., Möller, K., Shaw, G.M., Chiew, Y.S., and Benyo, B., Reconstructing asynchrony for mechanical ventilation using a hysteresis loop virtual patient model. *BioMedical Engineering OnLine* (2022). p. 16 DOI: 10.1186/s12938-022-00986-9.
36. Bates, J.H.T., *The linear single-compartment model*, in *Lung Mechanics: An Inverse Modeling Approach*, J.H.T. Bates, Editor. 2009, Cambridge University Press: Cambridge. p. 37-61.
37. Knopp, J.L., Chiew, Y.S., Georgopoulos, D., Shaw, G.M., and Chase, J.G., Ubiquity of models describing inspiratory effort dynamics in patients on pressure support ventilation. *IFAC Journal of Systems and Control* (2024). p. 100250 DOI: https://doi.org/10.1016/j.ifacsc.2024.100250.
38. Morton, S.E., Knopp, J.L., Tawhai, M.H., Docherty, P., Heines, S.J., Bergmans, D.C., Möller, K., and Chase, J.G., Prediction of lung mechanics throughout recruitment maneuvers in pressure-controlled ventilation. *Computer Methods and Programs in Biomedicine* (2020). p. 105696 DOI: https://doi.org/10.1016/j.cmpb.2020.105696.
39. Morton, S.E., Knopp, J.L., Chase, J.G., Möller, K., Docherty, P., Shaw, G.M., and Tawhai, M., Predictive Virtual Patient Modelling of Mechanical Ventilation: Impact of Recruitment Function. *Annals of Biomedical Engineering* (2019). p. 1626-1641 DOI: 10.1007/s10439-019-02253-w.
40. Sun, Q., Chase, J.G., Zhou, C., Tawhai, M.H., Knopp, J.L., Möller, K., Heines, S.J., Bergmans, D.C., and Shaw, G.M., Prediction and estimation of pulmonary response and elastance evolution for volume-controlled and pressure-controlled ventilation. *Biomedical Signal Processing and Control* (2022). p. 103367 DOI: https://doi.org/10.1016/j.bspc.2021.103367.
41. Docherty, P.D., Chase, J.G., Lotz, T.F., and Desaive, T., A graphical method for practical and

informative identifiability analyses of physiological models: a case study of insulin kinetics and sensitivity. *Biomed Eng Online* (2011). p. 39 DOI: 10.1186/1475-925X-10-39.
42. Knöbel, C., Schranz, C., and Möller, K., Identification of Models of Respiratory Mechanics - Influence of Parameter Estimation Techniques. *Biomed Tech.* (2011). p. 1-12.
43. Piquilloud, L., Vignaux, L., Bialais, E., Roeseler, J., Sottiaux, T., Laterre, P.-F., Jolliet, P., and Tassaux, D., Neurally adjusted ventilatory assist improves patient–ventilator interaction. *Intensive Care Medicine* (2011). p. 263-271 DOI: 10.1007/s00134-010-2052-9.
44. Moorhead, K., Piquilloud, L., Lambermont, B., Roeseler, J., Chiew, Y., Chase, J.G., Revelly, J.-P., Bialais, E., Tassaux, D., Laterre, P.-F., Jolliet, P., Sottiaux, T., and Desaive, T., NAVA enhances tidal volume and diaphragmatic electro-myographic activity matching: a Range90 analysis of supply and demand. *Journal of Clinical Monitoring and Computing* (2013). p. 61-70 DOI: 10.1007/s10877-012-9398-1.
45. Sinderby, C., Beck, J., Spahija, J., de Marchie, M., Lacroix, J., Navalesi, P., and Slutsky, A.S., Inspiratory muscle unloading by neurally adjusted ventilatory assist during maximal inspiratory efforts in healthy subjects. *Chest* (2007). p. 711-717 DOI: 10.1378/chest.06-1909.
46. Schmidt, M., Dres, M., Raux, M., Deslandes-Boutmy, E., Kindler, F., Mayaux, J., Similowski, T., and Demoule, A., Neurally adjusted ventilatory assist improves patient-ventilator interaction during postextubation prophylactic noninvasive ventilation. *Crit Care Med* (2012). p. 1738-44 DOI: 10.1097/CCM.0b013e3182451f77.
47. Chiew, Y.S., Piquilloud, L., Desaive, T., Lambermont, B., Roeseler, J., Revelly, J., Bialais, E., Tassaux, D., Jolliet, P., and Chase, J. *Effect of various Neurally adjusted ventilatory assist (NAVA) gains on the relationship between diaphragmatic activity (Eadi max) and tidal volume*. in *24th Annual Congress of the European Society of Intensive Care Medicine (ESICM 2011)*. 2011. Berlin, Germany.
48. Chiew, Y., Chase, J., Lambermont, B., Roeseler, J., Pretty, C., Bialais, E., Sottiaux, T., and Desaive, T., Effects of Neurally Adjusted Ventilatory Assist (NAVA) levels in non-invasive ventilated patients: titrating NAVA levels with electric diaphragmatic activity and tidal volume matching. *BioMedical Engineering OnLine* (2013). p. 61, http://www.biomedical-engineering-online.com/content/12/1/61.
49. Chiew, Y.S., Pretty, C., Docherty, P.D., Lambermont, B., Shaw, G.M., Desaive, T., and Chase, J.G., Time-varying respiratory system elastance: a physiological model for patients who are spontaneously breathing. *PLoS One* (2015). p. e0114847 DOI: 10.1371/journal.pone.0114847.
50. Zhou, C., Chase, J.G., Sun, Q., Knopp, J., Tawhai, M.H., Desaive, T., Möller, K., Shaw, G.M., Chiew, Y.S., and Benyo, B., Identification of Asynchronous Effect via Pressure-Volume Loop Reconstruction in Mechanically Ventilated Breathing Waveforms. *IFAC-PapersOnLine* (2021). p. 186-191 DOI: https://doi.org/10.1016/j.ifacol.2021.10.253.